

## Plasmon Dispersion and Anisotropy in Polymeric Sulfur Nitride, $(\text{SN})_x$

C. H. Chen\* and J. Silcox\*

*School of Applied and Engineering Physics, Cornell University, Ithaca, New York 14853*

and

A. F. Garito† and A. J. Heeger†

*Department of Physics and Laboratory for Research on the Structure of Matter, University of Pennsylvania, Philadelphia, Pennsylvania 19175*

and

A. G. MacDiarmid†

*Department of Chemistry and Laboratory for Research on the Structure of Matter, University of Pennsylvania, Philadelphia, Pennsylvania 19175*

(Received 2 October 1975)

Plasmon dispersion and anisotropy in the metallic polymer  $(\text{SN})_x$  were investigated directly by electron-energy-loss spectroscopy. A positive dispersion relation was observed for plasmons propagating along the polymer-chain  $b$  axis. As the plasmon wave vector changes from parallel to perpendicular to the  $b$  axis, the plasmon energy decreases from 2.5 to 1.5 eV consistent with the view that  $(\text{SN})_x$  is a poor conductor in the perpendicular direction rather than a quasi-one-dimensional metal.

In studies of one-dimensional metallic materials, a question of some considerable importance is that of distinguishing between such a system and an extremely anisotropic two- or three-dimensional conductor. A convenient attack on this problem can be made via electron-energy-loss experiments which can readily be exploited to give optical-anisotropy information. We report here such observations on polymeric  $(\text{SN})_x$ , a material initially thought to be quasi-one-dimensional<sup>1-3</sup> but which more recent optical-reflectivity measurements<sup>4</sup> have suggested is rather an anisotropic two- or three-dimensional conductor. Our observations, being direct measurements of the plasmon anisotropy and dispersion by high-energy (75-keV) inelastic electron scattering, provide further support for the latter view. Indeed some useful analogies have been made between the present studies and recent observations on graphite,<sup>5,6</sup> a uniaxial-layer-type crystal.

Bulk  $(\text{SN})_x$  single crystals were prepared as described previously.<sup>3,7</sup> Single-crystal films were obtained by cleaving the bulk crystal with sticky Teflon tape. The Cornell Hitachi-electron-microscope, Wien-electron-spectrometer system<sup>8</sup> was used to determine the energy-loss spectra with the microscope operated in the normal selected-area-diffraction mode. One advantage is that large-area specimens were not required: A sample area of linear dimension about a few thousand angstroms is sufficient for this arrangement with an energy resolution of  $\sim 0.5$  eV and a momentum-transfer resolution of  $\sim 0.95 \text{ \AA}^{-1}$ . Ex-

amination in the electron microscope revealed the characteristic fibrous structure of  $(\text{SN})_x$  while the single-crystal diffraction pattern indicated that both the  $b$  axis (the conducting axis) and the  $a$  axis lie in the plane of the film.<sup>9,10</sup> By rotating the diffraction pattern, electrons being scattered into different azimuthal planes are allowed to pass through the entrance slit of the spectrometer. Hence, energy-loss spectra can be recorded as a function of momentum transfer  $|\vec{q}|$  for different directions of the excitation wave vector  $\vec{q}$ ; i.e.,  $\vec{q}$  can be varied from a direction parallel to the conducting  $b$  axis to a perpendicular direction. The energy-loss spectra were recorded on photographic plates, and a Joyce-Loebl microdensitometer was then used to trace out the intensity maxima of the loss spectra on the plates.

Figure 1 shows the photograph of energy-loss spectra for  $q$  parallel to the  $b$  axis. The horizontal line at the bottom arises from electrons scattered by elastic collisions and by phonons. The sharp dispersive peak at  $\sim 2.5$  eV corresponds to the plasma excitations observed in the optical-reflectivity measurements which showed a well-defined plasma edge near 2.5 eV for the same polarization.<sup>3,4,11</sup> Two weaker peaks located at 6.6 and 8.7 eV are associated with interband transitions. These two peaks which occur only at small  $q$  are not clearly visible in Fig. 1 largely due to the rising instrumental background caused by electrons scattered off the entrance slit of the spectrometer; however, the microdensitometer

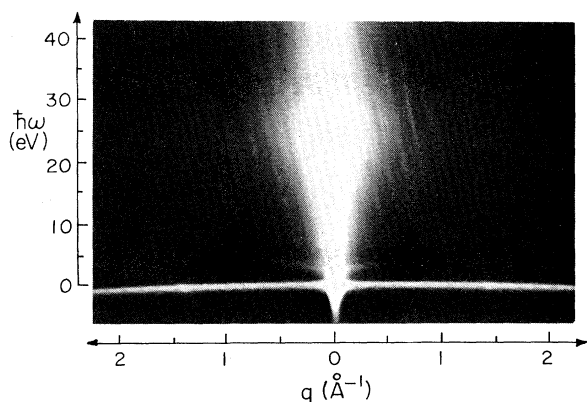


FIG. 1. Energy-loss spectrum of  $(\text{SN})_x$  ( $q$  parallel to the  $b$  axis) recorded on electron photographic plates. The spectrum shows intensity  $I(\omega, q)$  as a function of energy loss  $\hbar\omega$  and momentum transfer. The horizontal line at the bottom contains electrons scattered by elastic collisions and by phonons.

traces show these peaks easily. The optical-reflectivity measurements<sup>3,4,11</sup> also indicated that higher-energy interband transitions occur above the plasma edge. These interband transitions significantly affect the plasmon observed at 2.5 eV. A large broad peak near 23 eV is also observed. This is the plasmon involving all valence electrons (eleven electrons per SN molecule and four SN molecules per unit cell) in the  $(\text{SN})_x$  crystal, analogous to the  $\pi + \sigma$  plasmons observed in graphite.<sup>5,6</sup> Assuming the plasmon energy exceeds the interband transitions, the free-electron approximation can be used,  $\omega_p = (4\pi n e^2 / m)^{1/2}$  with  $n = 3.3 \times 10^{23} \text{ cm}^{-3}$ . The plasma energy,  $\hbar\omega_p = 21.3 \text{ eV}$ , is close to the large peak observed near 23 eV. These values reflect the wide energy separation between the valence plasma excitations and the lower-energy interband transitions which lead to only a relatively small shift of  $\omega_p$ . We note that the intensity profile of this 23-eV peak is not symmetric with the steeper slope on the high-energy side. This is probably caused by some unresolved broad excitations on the lower side of the peak.

The important feature in the parallel loss spectra (Fig. 1) is the 2.5-eV plasmon peak, somewhat analogous to the  $\pi$  plasmons observed in graphite.<sup>5,6</sup> The measured dispersion of this peak for  $q$  parallel to the  $b$  axis is shown in Fig. 2. As is commonly observed in ordinary metals, the dispersion relation is positive, in contrast to recent plasmon-dispersion measurements of the quasi-one-dimensional metal TTF-TCNQ (tetrathiafulvalene-tetracyanoquinodimethane) where a

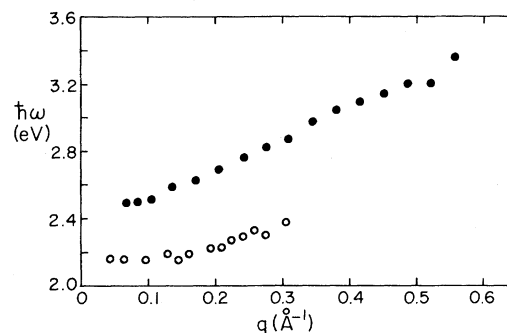


FIG. 2. Dispersion of plasmons in  $(\text{SN})_x$ . Plasmons propagating along the conducting  $b$  axis are represented by closed circles and plasmons propagating at  $50^\circ$  to the  $b$  axis by open circles.

negative plasmon dispersion was reported.<sup>12</sup> The plasmon dispersion (Fig. 2) starts with  $\hbar\omega = 2.48 \text{ eV}$  at  $q = 0$  and extends to  $3.4 \text{ eV}$  at  $q \approx 0.55 \text{ \AA}^{-1}$ . The measured dispersion curve follows closely the well-known relation  $\omega = \omega_p + \alpha(\hbar/m)q^2$ , with  $\hbar\omega_p = 2.48 \text{ eV}$  and  $\alpha = 0.62$  for  $q < 0.3 \text{ \AA}^{-1}$ . At larger  $q$ , (where local-field effects<sup>13</sup> may no longer be negligible), the measured data points fall below this simple theoretical expression. We note that the plasmon-dispersion coefficient  $\alpha$  for  $(\text{SN})_x$  is significantly larger than the corresponding  $\alpha$  values observed in most metals ( $\alpha \sim 0.4$ ).<sup>14</sup> The plasmon energy at  $q = 0$  also agrees with the value obtained from optical measurements<sup>3,4</sup> which correspond on a best-fit basis to a point where  $\epsilon(\omega) = 0$ , i.e.,  $\hbar\omega_p = 2.5 \text{ eV}$ . Assuming that there is only one  $\pi$  electron per molecule participating in the plasma oscillation, the free-electron plasmon energy should be  $6.43 \text{ eV}$ . The major contribution to the shift of the plasmon energy from its free-electron value can be attributed to the two interband transitions located at  $6.6$  and  $8.7 \text{ eV}$ . It is well known that interband transitions which are higher in energy than the free-electron plasmon energy will act to move the plasmon down to lower energies, whereas those which occur at lower energy act to push the plasmon energy up.<sup>15</sup> In the early reflectivity study of  $(\text{SN})_x$ ,<sup>3</sup> interband effects were suggested and subsequently verified by further extensive optical measurements.<sup>4,11</sup>

The width of the plasmon at  $2.48 \text{ eV}$  obtained by optical measurements is about  $0.3 - 0.5 \text{ eV}$ . In the present studies, the observed plasmon peak is at least as narrow as the experimental energy resolution ( $0.5 \text{ eV}$ ).

Direct measurements of the optical anisotropy were obtained by recording energy-loss spectra

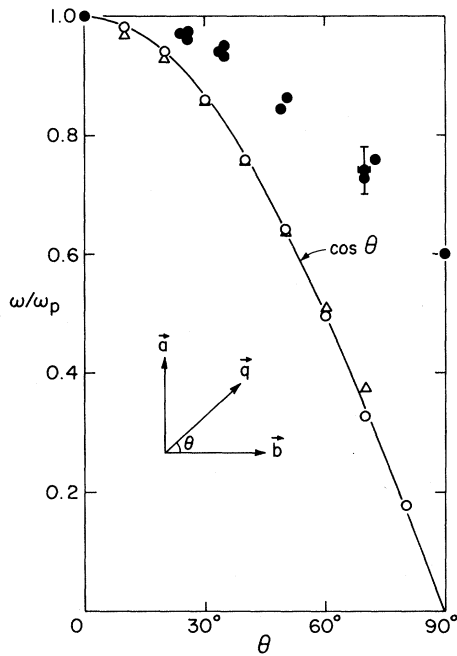


FIG. 3. Angular dependence of plasmon energy in  $(\text{SN})_x$  (represented by closed circles). The plasmon energy at each angle  $\theta$  is measured at  $q \approx 1 \text{ \AA}^{-1}$ . The precision with which the position of a "stand-alone" peak can be determined is  $\sim \pm 0.1 \text{ eV}$ . For comparison, plasmon anisotropy is also calculated for TTF-TCNQ (triangles) and KCP (open circles) using the dielectric constants obtained from reflectivity data (Refs. 16 and 17).

for  $\vec{q}$  at an angle to the polymer-chain  $b$  axis, but still in the  $\vec{a}$ - $\vec{b}$  plane. The energy-loss spectra for  $\vec{q}$  perpendicular to the  $b$  axis were obtained by collecting those electrons scattered along the  $a$  axis. Comparisons with the loss spectra for  $\vec{q}$  parallel to the  $b$  axis show that the plasmon energy and dispersion are anisotropic. Specifically, the sharp strong plasmon peak at 2.48 eV for  $\vec{q}$  parallel to the  $b$  axis is now shifted to 1.5 eV and is considerably weakened and broadened. No significant anisotropy was observed for the higher-energy excitations. We believe that the 1.5-eV peak is a plasmon since it can be followed as a continuous function of  $\theta$ , the angle between  $\vec{q}$  and the  $b$  axis, from the  $b$ -axis plasmon to the  $a$ -axis plasmon (see Fig. 3). Both the parallel and perpendicular data are consistent with the plasma-like edges observed optically.<sup>4</sup> The plasmon dispersion also varies continuously with  $\theta$  decreasing to little or no dispersion at  $90^\circ$ . We show dispersion for  $\theta = 50^\circ$  in Fig. 2. The broad plasma edge observed in the transverse optical reflectance is broadened by scattering because of the fibrous and disordered structure character-

istic of  $(\text{SN})_x$  samples in the transverse direction in addition to normal scattering processes. In itself, this observation indicates metallic behavior for  $(\text{SN})_x$  in the transverse direction and, therefore, is evidence that  $(\text{SN})_x$  is an anisotropic three-dimensional metal rather than one dimensional.

The significance of the data given in Fig. 3 can, however, be explored further. The observed angular variation is less than the cosine dependence,  $\hbar\omega(\theta) = \hbar\omega(0) \cos\theta$ , predicted by a recent random-phase-approximation calculation of the frequency- and wave-vector-dependent dielectric function for a quasi-one-dimensional metal.<sup>18</sup> In the case of an anisotropic crystal, the scattering cross section for high-energy electrons is proportional to the energy-loss function<sup>19</sup>  $\text{Im}(1/\vec{q} \cdot \vec{\epsilon} \cdot \vec{q})$  where  $\vec{\epsilon}(q, \omega)$  is the dielectric tensor. For a uniaxial crystal this loss function can be written in terms of the principal components in the parallel and perpendicular directions,  $\epsilon_{\parallel}$  and  $\epsilon_{\perp}$ , and  $\theta$ , as  $\text{Im}(\epsilon_{\parallel} \cos^2\theta + \epsilon_{\perp} \sin^2\theta)^{-1}$ . In the present case  $\epsilon_{\parallel}$  is clearly metallic and the question is whether  $\epsilon_{\perp}$  is metallic or insulating. For example, in both TTF-TCNQ<sup>16</sup> and  $\text{K}_2[\text{Pt}(\text{CN})_4]\text{Cl}_{0.3} \cdot 3\text{H}_2\text{O}$  (KCP),<sup>17</sup>  $\epsilon_{\perp}(\omega)$  is positive and slowly varying in the energy range of interest, behavior which has been interpreted in terms of diffusive electron hopping between individual chains.<sup>16</sup> The simplest model is  $\epsilon_{\parallel} = 1 - \omega_{p\parallel}^2/\omega^2$  and  $\epsilon_{\perp} = 1 + P(\omega)$ , where  $P(\omega)$  is  $-\omega_{p\perp}^2/\omega^2$  for a metal,  $-\omega_{p\perp}^2\tau_{\perp}^2$ , where  $\omega_{p\perp}^2\tau_{\perp}^2 < 1$ , for an overdamped metal (with a mean free path much less than a lattice constant), or  $\alpha$  (a positive constant) for an insulator. Taking the plasmon energy as the root,  $\omega(\theta)$ , of  $\epsilon_{\parallel} \cos^2\theta + \epsilon_{\perp} \sin^2\theta = 0$ , we find that for the metallic form  $\hbar\omega(\theta) = \hbar(\omega_{p\parallel}^2 \cos^2\theta + \omega_{p\perp}^2 \sin^2\theta)^{1/2} \geq \hbar\omega_{p\parallel} \cos\theta$  and for the insulating form  $\hbar\omega(\theta) = \hbar\omega_{p\parallel} \cos\theta(1 + \alpha \sin^2\theta)^{-1/2} \leq \hbar\omega_{p\parallel} \cos\theta$ . This suggests that the Williams and Bloch expression<sup>18</sup>  $\hbar\omega(\theta) = \hbar\omega(0) \cos\theta$  marks the transition between metallic and insulating behavior. This clearly has to be treated with some caution for real materials which are apt to be somewhat more complex but nevertheless can generate useful insight. We have evaluated the energy-loss function for both TTF-TCNQ and KCP from dielectric data (including damping) obtained from reflectivity measurements<sup>16,17</sup> (see Fig. 3). For both TTF-TCNQ and KCP the values for the plasmon peak lie surprisingly close to the  $\cos\theta$  curve.<sup>20</sup> The plasmon peak for TTF-TCNQ as determined from  $\text{Re}(\epsilon) = 0$  lies below  $\cos\theta$ . In both materials, structure occurs in the  $\epsilon_{\parallel}$  for  $\omega \ll \omega_p$  which results in modification of the simple

model given above. Nevertheless, the contrast between  $(SN)_x$  and the two other one-dimensional candidates is marked.

In conclusion, we have presented direct measurements of the plasmon dispersion and optical anisotropy in single crystal  $(SN)_x$ . The observed data confirm the good metallic behavior along the chain direction. In the perpendicular direction,  $(SN)_x$  has the dielectric function of a poor metal in contrast to TTF-TCNQ where the transverse optical properties show no sign of metallic behavior.<sup>16</sup> Thus, the energy-loss experiments suggest that  $(SN)_x$  should not be viewed as a one-dimensional metal but rather as an anisotropic two- or three-dimensional conductor.

The authors thank Dr. C. M. Mikulski for aid in sample preparation, and acknowledge helpful correspondence with Dr. A. J. Epstein and Dr. J. J. Ritsko.

---

\*Work supported by the National Science Foundation and the Advanced Research Projects Agency through the Cornell Materials Science Center.

†Work supported in part by the National Science Foundation through Grant No. GH-37250 of the Laboratory for Research on the Structure of Matter, and Grants No. GH-39303, and No. GP-41764x, and by the Advanced Research Projects Agency through Grant No. DAHC-15-72-C-0174.

<sup>1</sup>V. V. Walatka, Jr., M. M. Labes, and J. H. Perlstein, *Phys. Rev. Lett.* **31**, 1139 (1973); C. H. Hsu and M. M. Labes, *J. Chem. Phys.* **61**, 4640 (1974).

<sup>2</sup>R. L. Greene, P. M. Grant, and G. B. Street, *Phys. Rev. Lett.* **34**, 89 (1975); R. L. Greene, G. B. Street, and L. J. Suter, *Phys. Rev. Lett.* **34**, 577 (1975).

<sup>3</sup>A. A. Bright, M. J. Cohen, A. F. Garito, A. J. Heeger, C. M. Mikulski, P. J. Russo, and A. G. MacDiarmid, *Phys. Rev. Lett.* **34**, 206 (1975).

<sup>4</sup>A. A. Bright, M. J. Cohen, A. F. Garito, A. J. Heeger, C. M. Mikulski, and A. G. MacDiarmid, *Appl.*

*Phys. Lett.* **26**, 612 (1975), and to be published.

<sup>5</sup>K. Zeppenfeld, *Z. Phys.* **211**, 391 (1968).

<sup>6</sup>C. H. Chen and J. Silcox, *Phys. Rev. Lett.* **35**, 390 (1975).

<sup>7</sup>C. M. Mikulski, P. J. Russo, M. S. Saran, A. G. MacDiarmid, A. P. Garito, and A. J. Heeger, to be published.

<sup>8</sup>G. H. Curtis and J. Silcox, *Rev. Sci. Instrum.* **42**, 630 (1971).

<sup>9</sup>M. Boudeulle, A. Douillard, P. M. Michel, and G. Vallet, *C. R. Acad. Sci., Ser. C* **272**, 2137 (1971); M. Boudeulle, *Cryst. Struct. Commun.* **4**, 9 (1975).

<sup>10</sup>M. J. Cohen, A. F. Garito, A. J. Heeger, A. G. MacDiarmid, and M. S. Saran, to be published.

<sup>11</sup>L. Pintschovius, H. P. Gesserich, and W. Moller, *Solid State Commun.* **17**, 477 (1975); P. M. Grant, R. L. Greene, and G. B. Street, to be published.

<sup>12</sup>J. J. Ritsko, D. J. Sandman, A. J. Epstein, P. C. Gibbons, S. E. Schnatterly, and J. Fields, *Phys. Rev. Lett.* **34**, 1330 (1975).

<sup>13</sup>S. L. Adler, *Phys. Rev.* **126**, 413 (1962).

<sup>14</sup>H. Raether, in *Ergebnisse der exakten Naturwissenschaften*, edited by S. Flugge, F. Trendelenburg, and F. Hund (Springer, Berlin, 1965), Vol. 35, p. 85.

<sup>15</sup>D. Pines, *Elementary Excitations in Solids* (Benjamin, New York, 1963).

<sup>16</sup>A. A. Bright, A. F. Garito, and A. J. Heeger, *Phys. Rev. B* **10**, 1328 (1974); C. S. Jacobsen, D. B. Tanner, A. F. Garito, and A. J. Heeger, *Phys. Rev. Lett.* **33**, 1559 (1974).

<sup>17</sup>J. Bernasconi, P. Bruesch, D. Kuse, and H. R. Zeller, *J. Phys. Chem. Solids* **35**, 145 (1974).

<sup>18</sup>P. F. Williams and A. N. Bloch, *Phys. Rev. B* **10**, 1097 (1974).

<sup>19</sup>J. Hubbard, *Proc. Phys. Soc., London* **58**, 976 (1955).

<sup>20</sup>The existing electron-energy-loss data on TTF-TCNQ (Ref. 12) are consistent with these loss profiles if intensity dependence on  $\theta$  is taken into account. Convolution of a cylindrical Gaussian weighting function in  $q$  with a linear intensity change with  $\theta$  based on the loss profiles gives a value for  $\omega_p(45^\circ)$  which is within experimental uncertainty of the measured value; A. J. Epstein and J. J. Ritsko, private communication.

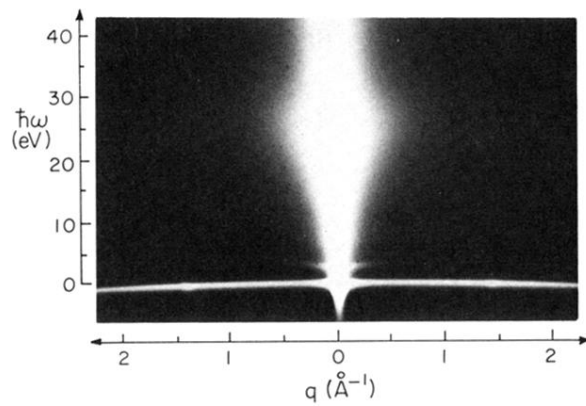


FIG. 1. Energy-loss spectrum of  $(\text{SN})_x$  ( $q$  parallel to the  $b$  axis) recorded on electron photographic plates. The spectrum shows intensity  $I(\omega, q)$  as a function of energy loss  $\hbar\omega$  and momentum transfer. The horizontal line at the bottom contains electrons scattered by elastic collisions and by phonons.